

Supporting Information

An Empirical Optimization of Peptide Sequence and Nanoparticle Colloidal Stability: The Impact of Surface Ligands and Implications for Colorimetric Sensing

Zhicheng Jin,^{a,†} Justin Yeung,^{b,†} Jiajing Zhou,^a Maurice Retout,^a Wonjun Yim,^c Pavla Fajtová,^d Bryan Gosselin,^{e,f} Ivan Jabin,^e Gilles Bruylants,^f Hedi Mattoussi,^g Anthony J. O'Donoghue,^d and Jesse V. Jokerst^{a,c,h*}

^aDepartment of NanoEngineering, University of California, San Diego, La Jolla, CA 92093, United States

^bDepartment of Bioengineering, University of California San Diego, La Jolla, CA 92093, United States

^cMaterials Science and Engineering Program, University of California, San Diego, La Jolla, CA 92093, United States

^dSkaggs School of Pharmacy and Pharmaceutical Sciences, University of California, San Diego, La Jolla, CA 92093, United States

^eLaboratoire de Chimie Organique, Université libre de Bruxelles (ULB), avenue F. D. Roosevelt 50, CP160/06, B-1050 Brussels, Belgium

^fEngineering of Molecular NanoSystems, Ecole Polytechnique de Bruxelles, Université libre de Bruxelles (ULB), avenue F. D. Roosevelt 50, CP165/64, B-1050 Brussels, Belgium

^gDepartment of Chemistry and Biochemistry, Florida State University, Tallahassee, FL 32306, United States

^hDepartment of Radiology, University of California, San Diego, La Jolla, CA 92093, United States

*Corresponding author's email: jjokerst@ucsd.edu (J.V.J.)

† Z.J. and J.Y. contributed equally to this work.

Table of Content

1. Materials	S3
2. Instrumentations and Characterizations	S4
2.1 Citrate-AuNP synthesis.	S4
2.2 Peptide synthesis.	S4
2.3 Proteolysis of peptide.	S5
3. Surface Functionalization	S5
3.1 Ligand exchange.	S5
3.2 Nanoparticle characterization.....	S6
3.3 Agarose gel electrophoresis.	S6
4. Stability Test in Various Chemical Environments	S7
4.1 Ionic environment	S7
4.2 Thiolate (redox-rich) environment.	S7
4.3 Hydrophobic (aromatic-rich) environment	S7
5. AuNP Aggregation Propensity with M ^{Pro} -substrate Segments	S7
5.1 Charged SGFRGGRGG	S7
5.2 Thiolate SGFACGAGC	S8
5.3 Aromatic SGFFPC	S8

6. Probe Interparticle Interactions.....	S8
7. Working Window (or Dynamic Range) Determination.....	S8
8. LoD measurement.....	S9
9. References.....	S9
Figure S1. TEM images of the representative AuNPs.....	S11
Figure S2. Hydrodynamic diameter (D_H) distributions obtained from dynamic light scattering of ligated AuNPs.....	S12
Figure S3. Absorption spectra of AuNPs capped with different ligands when incubated with various concentrations of NaCl.....	S13
Figure S4. Absorption spectra of AuNPs capped with different ligands when incubated with various concentrations of dithiothreitol (DTT).....	S14
Figure S5. Absorption spectra of AuNPs capped with different ligands when incubated with various concentrations of amphiphilic FFPC.....	S15
Figure S6. HPLC and ESI-MS data of the peptide segments	S16
Figure S7. Time-dependent aggregation kinetics	S17
Figure S8. Concentration-dependent absorbance ratio (Abs_{600}/Abs_{520}) of the ligated AuNPs after incubating with the EF, TF, and AF peptides.....	S18
Figure S9. The choice of a peptide/AuNP pair as a good color sensor	S19
Figure S10. Working window of Mega peptide.....	S20
Figure S11. ESI-MS data of intact Mega peptide and the stability of BSPP-AuNPs in different matrix media.	S21
Figure S12. Dilution factor required for color changes in 1% BSA and human plasma.....	S22
Figure S13. Concentration optimization of the 13-nm AuNPs for aggregation-based colorimetric assays.....	S22

1. Materials

Sodium citrate tribasic dihydrate (>99%), gold(III) chloride trihydrate ($\text{HAuCl}_4 \cdot 3\text{H}_2\text{O}$, >99.9%), sodium dodecyl sulfate (SDS, >99%), Trizma[®] base (>99.9%), Trizma[®] hydrochloride (>90%), tris(2-carboxyethyl)phosphine hydrochloride (TCEP-HCl), bis(p-sulfonatophenyl)phenylphosphine dihydrate dipotassium salt (BSPP, 97%), DL-dithiothreitol (DTT, >99%), (-)-epigallocatechin gallate (EGCG, >95%), tannic acid (TA, ACS reagent), sodium 3-mercaptopropionate (MPS, 90%), poly(acrylic acid, sodium salt) solution (PAA, average Mw ~15,000, 35 wt% in H_2O), poly(sodium 4-styrenesulfonate) (PSS, average Mw ~70,000), polyvinylpyrrolidone (PVP, average Mw ~40,000), urea (99%), bovine serum albumin (>96%), glycerol (>99%), trifluoroacetic acid (TFA, HPLC grade, >99%), 2,2'-(ethylenedioxy)diethanethiol (EDDET, 95%), and piperidine (ReagentPlus[®], 99%) were purchased from Sigma Aldrich (St Louis, MO). The 3-mercaptopropionic acid (MPA, 99%) was from ThermoFisher Scientific (Waltham, MA). Sodium diphenylphosphinobenzene-3-sulfonate (DPPS, >90%), thioanisole (>99%), N,N-diisopropylethylamine (DIPEA, >99%), and triisopropylsilane (TIPS, >98%) were purchased from Tokyo Chemical Industry Co., Ltd. (TCI). Reduced glutathione (GSH, $\geq 98\%$) was from MP Biomedicals (Santa Ana, CA). Fmoc-protected amino acids, hexafluorophosphate benzotriazole tetramethyl uronium (HBTU), and Fmoc-rink amide MBHA resin (0.67 mmol/g, 100-150 mesh) were purchased from AAPPTec, LLC (Louisville, KY). The recombinant SARS-CoV-2 main protease (M^{pro}) was expressed using the M^{pro} plasmid provided by Prof. Rolf Hilgenfeld, University of Lübeck, Germany and purified as previously described.¹⁻² The purified M^{pro} was stored at $-80\text{ }^\circ\text{C}$ in 20 mM Tris-HCl, pH 8.0, 150 mM NaCl, 1 mM DTT, 5% glycerol. TBE buffer (10 \times , molecular biology certified) was from IBI Scientific, Inc (Dubuque, IA). A 10-mL disposable reaction vessel and the pressure caps for peptide-resin cleavage were purchased from Torviq Inc. (Tucson, AZ). The PD-10 desalting columns containing Sephadex G-25 resin (particle size <50 μm) were from GE Healthcare (Chicago, IL). The lipoic acid (LA)-ligands such as LA-ZW, LA-PEG-OCH₃, LA-PEG-COOH, and LA-PIMA-PEG-OCH₃ were synthesized following our previous protocol.³ The C₄X₄-AuNPs were synthesized following our previous protocol [PMC8340414]. Organic solvents including N,N-dimethylformamide (DMF, sequencing grade), acetonitrile (ACN, HPLC grade), ethyl ether (certified ACS), methylene chloride (DCM, certified ACS), and dimethyl sulfoxide (DMSO, certified ACS) were also from Fisher Scientific International, Inc. (Hampton, NH). Ultrapure water (18 M Ω ·cm) was obtained from a Milli-Q Academic water purification system (Millipore

Corp., Billerica, MA). TEM grids (formvar/carbon 300 mesh Cu) were purchased from Ted Pella (Redding, CA). The Amicon[®] ultra-15 centrifugal filter units (Mw cutoff =100 kDa) and automation compatible syringe filters (hydrophilic PTFE, 0.45 μm) were from MilliporeSigma (St. Louis, MO). Glassware and stir bars were cleaned with aqua regia ($\text{HCl}:\text{HNO}_3=3:1$ by volume) and boiling DI water before use.

2. Instrumentations and Characterizations

2.1 Citrate-AuNP synthesis. The citrate-AuNPs (~13 nm in diameter by TEM, **Fig. S1**) were prepared using the Turkevich method⁴ by rapidly injecting an aqueous solution of sodium citrate tribasic dihydrate (150 mg, 5 mL) into an aqueous solution of $\text{HAuCl}_4 \cdot 3\text{H}_2\text{O}$ (45 mg, 300 mL) under boiling conditions and vigorous stirring. The reaction mixture was left boiling while stirring for another 20 min and then cooled to room temperature. The deep red dispersion was then purified by applying one round of centrifugation at 18,000 g for 30 min, and the supernatant was discarded. The resulting pellet of citrate-AuNPs was redispersed in DI water by sonication, passed through the automation-compatible syringe filters (*i.e.*, hydrophilic PTFE, 0.45 μm), and stored at ambient conditions ($\epsilon_{520}=4.0 \times 10^8 \text{ M}^{-1} \text{ cm}^{-1}$).⁵

2.2 Peptide synthesis. Peptides were synthesized using an automated Eclipse[™] peptide synthesizer (AAPPTec, Louisville, KY) through standard solid phase Fmoc synthesis on Rink-amide resin. Peptides were chain assembled by Fmoc-SPPS (solid-phase peptide synthesis) on rink-amide-MBHA-resin (0.67 mmol/g, 200 mg) using an automated Eclipse[™] peptide synthesizer (AAPPTec, Louisville, KY). Amino acid couplings were performed under the protection of nitrogen with 0.2 M Fmoc-amino acid (5 *equiv.*) in 3 mL DMF, 0.2 M HBTU in DMF (5 *equiv.*) in 3 mL DMF, 0.3 M DIPEA (7.5 *equiv.*) in 3 mL DMF, and 20% (v/v) piperidine in 2 \times 4 mL DMF for each cycle. The number of coupling cycles was based on the sequence analysis software tool (AAPPTec). The resulting peptides on the resin were transferred into a syringe filter (Torviq Inc.), washed with five rounds of DCM (2 mL each), and dried under vacuum. The peptides were then cleaved from the resin using a cleavage cocktail (3 mL) that contained TFA (82.5%), EDDT (2.5%), phenol (5%), thioanisole (5%), and H_2O (5%). Resins were treated with the cleavage cocktail for 3 h with gentle shaking. After cleavage, the resin was filtered, and the filtrate containing the crude peptides was precipitated/washed with three rounds of cold ether (15 mL, $-20 \text{ }^\circ\text{C}$), suspended in 50% ACN/ H_2O (10 mL, v/v), and lyophilized in a FreeZone Plus 2.5 freeze dry system (Labconco

Corp., Kansas, MO).

Peptide purification used a Shimadzu LC-40 HPLC system equipped with a LC-40D solvent delivery module, a photodiode array detector SPD-M40, and DGU-403 degassing unit. The crude sample was dissolved in an acetonitrile/H₂O mixture (1:1, v/v) with an injection volume of 2 mL on a Zorbax 300 BS, C18 column (5 mm, 9.4×250 mm) from Agilent (Santa Clara, CA), and eluted at a flow rate of 1.5 mL/min over a 40 min linear gradient from 10% to 95% of acetonitrile in water (with 0.05% TFA, HPLC grade). Preparative injections were monitored at 190, 220, and 254 nm. Fractions containing the pure peptide as confirmed by electrospray ionization mass spectroscopy (ESI-MS) were lyophilized and aliquoted. Peptide synthesis and cleavage were also confirmed using ESI-MS (positive ion mode) *via* the Micromass Quattro Ultima mass spectrometer in the Molecular MS Facility (MMSF) at UC San Diego. ESI-MS samples were prepared in a MeOH/H₂O mixture (1:1, v/v).

The peptide concentration was determined using a NanoDrop™ One UV-vis spectrophotometer (Thermo Fisher Scientific, Waltham, MA): The 31-method was applied for peptide quantification.⁶ The absorption coefficient of $\epsilon_{205} = 31 \text{ mL}\cdot\text{mg}^{-1}\cdot\text{cm}^{-1}$ was used (note that DMSO or acetonitrile contributes absorbance signal at 205 nm; thus, water or alcohol is used as the solvent blank).⁷⁻⁸

2.3 Proteolysis of peptide. A peptide solution (500 μL , 1 mg/mL, DMSO <1% v/v) in phosphate buffer (10 mM, pH 8.0) was incubated with M^{pro} at a molar ratio of 3000:1 (substrate: enzyme) at 37 °C for overnight to make a peptide fragment solution. To confirm the M^{pro} cleavage site, the mixture above was applied on a Shim-pack GIS, C18, analytical column (5 μm , 4.6×100 mm) from Agilent and eluted at a flow rate of 1 mL/min with a 40-minute gradient from 10% to 95% acetonitrile in DI water (with 0.05% TFA, HPLC grade). Preparative injections were monitored at 190, 220, and 254 nm. All fractions were collected, and the eluent's molecular weight was determined using an ESI-MS spectrometer.

3. Surface Functionalization

3.1 Ligand exchange. Each ligand solution (in DI water) was added to individual scintillation vials containing citrate-AuNPs (10 mL, 3.4 nM) equipped with a stir bar under sonication. The molar ratio of ligand (or monomer)-to-AuNP is set to 130,000 unless otherwise specified (see below). This molar ratio for some ligands was optimized to be: TA (13,000), GSH (13,000), DTT (3,000,000), LA-ZW (13,000), LA-PIMA-PEG (1,300), and BSA (4,000). These

mixtures were stirred at 700 RPM for 18 h at room temperature. The resulting gold colloids were purified from the excess ligands using Amicon ultra-15 centrifugal filter units (Mw cutoff =100 kDa) *via* two rounds of dilution/concentration at 5,000 RPM for 5-10 min. The Au pellet was then retrieved, redispersed/sonicated in 10 mL DI water, and stored at 4 °C for further use.

Remark: Modified procedures were applied for few ligations to avoid irreversible aggregation, *e.g.*, the ligation time for TCEP, MPS, MPA was set to 5 h, 3 h, and 30 min, respectively; the MPS- and MPA-AuNPs were sequentially exchanged from BPP-AuNPs (as the intermediate). The X₄C₄ ligand is modified upon reduction and NP synthesis *in situ* without ligand exchange, and it is grafted through covalent Au-C bonds.

3.2 Nanoparticle characterization. The optical absorption measurements were collected using a hybrid multi-mode microplate reader (Synergy™ H1 model, BioTek Instruments, Inc.) in a 96-well plate. The dynamic light scattering (DLS) and zeta potential (ζ) measurements were carried out using a compact Zetasizer Nano ZS90 (Malvern Panalytical, Inc.). The ligated AuNPs were prepared in DI water for DLS measurements. Transmission electron microscopy (TEM) images of the Au colloids were acquired using a JEOL 1200 EX II operating at 80 kV. The TEM grids were prepared by drop casting samples in water (4 mL) followed by natural drying.

3.3 Agarose gel electrophoresis. Gel electrophoresis measurements were applied side-by-side to the AuNPs modified with different surface ligands. They were conducted on a 0.7% (w/v) agarose gel prepared in 100 mL of TBE buffer (0.5×). Here, 47- μ L aliquots of the ligated AuNPs (10 nM) were mixed with 3 μ L of glycerol (6%, v/v). They were then homogenized and loaded into the gel wells. An initial 13 V/cm electric field was applied for 20 s followed by running at 6.5 V/cm for 30 min. Photographic images were taken by smartphone in a professional lightbox.

According to Ferguson analysis⁹, the relationship between electrophoretic mobility (M) and gel concentration (T) is given by:

$$\log_{10} M = \log_{10} M_0 - K_R T \quad (S1)$$

where M_0 is the particle mobility in absence of gel (*i.e.*, in solution). The retardation coefficient, K_R , is strongly dependent on both particle size and charge due to the particle interactions with the gel network. For low-concentration gels, such as those made of one-dimensional fiber polymers such as agarose, $\sqrt{K_R}$ varies linearly with the particle size⁹

$$\sqrt{K_R} = AR_{eff} + B \quad (S2)$$

where R_{eff} is the effective radius of the particle (similar to the geometric radius), and A and B are constant parameters that depend on the gel network characteristics and experimental conditions (e.g., buffer, temperature, and applied electric field).

4. Stability Test in Various Chemical Environments

4.1 Ionic environment.¹⁰ Next, 20 μ L of NaCl solutions at various concentrations (e.g., 0, 10, 20, 50, 100, 200, 500, and 1000 mM) were loaded in a 96-well plate. Each ligand-capped AuNPs (3.4 nM, 100 μ L) was then added to the well and thoroughly mixed. The resulting absorbance spectrum for each mixture at 10 min was recorded in a hybrid multi-mode microplate reader (Synergy™ H1 model, BioTek Instruments, Inc.); measurements were done in duplicate. The absorbance ratio of Abs₆₀₀/Abs₅₂₀ was then extracted, averaged, and plotted against NaCl concentration; the standard error of means was represented as error bars.

4.2 Thiolate (redox-rich) environment.³ Various amounts of DTT solution were mixed with 1.2 μ L of NaCl solution (1 M), and DI water was added to adjust the volume to 20 μ L for a final concentration of 0, 1, 2, 5, 10, 20, 50 100 μ M DTT in a 96-well plate,. The different ligand-capped AuNPs (3.4 nM, 100 μ L) were then added to the well and thoroughly mixed. The resulting absorbance spectrum for each mixture at 10 min was recorded; measurements were done in duplicate. The absorbance ratio of Abs₆₀₀/Abs₅₂₀ was then extracted, averaged, and plotted against NaCl concentration; the standard error of means was represented as error bars.

4.3 Hydrophobic (aromatic-rich) environment. The procedure above was repeated for FFPC solutions at various concentrations. e.g., 0, 5, 10, 20 50, 100, 200, 500 μ M.

5. AuNP Aggregation Propensity with M^{Pro}-substrate Segments

5.1 Charged SGFRGGRGG.⁷ Next, 20 μ L of SGFRGGRGG peptide solutions at various concentrations (0.1, 0.2, 0.5, 1, 2, 5, 10, 20, 50, 100 μ M) were loaded in a 96-well plate. Each ligand-capped AuNPs (3.4 nM, 100 μ L) was then added to the well and thoroughly mixed. The ratiometric absorbance data (Abs₆₀₀/Abs₅₂₀) were recorded over 1 h with 1 min intervals between each cycle in a hybrid multi-mode microplate reader (Synergy™ H1 model, BioTek Instruments, Inc.). Measurements were done in duplicate. The absorbance ratios were averaged

and plotted against NaCl concentration; the standard error of means was represented as error bars.

5.2 Thiolate SGFACGAGC.⁸ The procedure above was repeated for SGFACGAGC peptide.

5.3 Aromatic SGFFPC. The procedure above was repeated for SGFFPC peptide.

6. Probe Interparticle Interactions

A 0.5-mL microtube AuNP dispersion (100 μ L, 3.4 nM) was thoroughly mixed with the corresponding peptide solution (e.g., charged SGFRGGRGG 2.4 μ L, 1.62 mM) until there was no further color change. The mixture was then mildly centrifuged at 500 g for 1 min, and the supernatant was discarded. The pellet was then added with the probing solution (100 μ L) and sonicated for 10 s including DI water, PEG₂₀₀₀ (10 mM), Triton X-100 (10 mM), HCl (10 mM), NaOH (10 mM), NaCl (10 mM), Urea (1 M), SDS (10 mM), DMSO (100%), DMF (100%), sodium citrate tribasic (10 mM), and the coating ligand solution (10 mM). Ratiometric absorbance data (Abs_{600}/Abs_{520}) were collected in a hybrid multi-mode microplate reader (Synergy™ H1 model, BioTek Instruments, Inc.) in a 96-well plate. The negative and positive controls used gold nanoparticle only and particle dispersions with peptide fragments, respectively.

Remark: Based on the screening results from **Figure 3a**, BSPP-AuNPs were selected to test with charged SGFRGGRGG peptide solution; citrate-AuNPs were chosen to test with both thiolate SGFACGAGC and aromatic SGFFPC peptide solutions. The peptide solutions used to aggregate AuNPs via thiolate and aromatic interactions were 1 μ L, 980 μ M and 10 μ L, 6.2 mM respectively.

7. Working Window (or Dynamic Range) Determination

The intact Mega (DDDTSAVLQSGFFRCRPC) peptide was dissolved in phosphate buffer (10 mM, pH 8.0, DMSO < 1% v/v) for use. The peptide fragments were prepared by incubating the corresponding intact peptide with M^{PtO} at a molar ratio of 3000:1 at 37 °C for overnight (see **Section 2.3, SI**). Next, BSPP-AuNPs (100 μ L, 3.4 nM) were mixed with the intact or fragmented peptides (20 μ L) in a 96-well plate to reach final concentrations of 0.1, 0.2, 0.5, 1, 2, 5, 10, 20, and 50 μ M. Data were collected in a hybrid multi-mode microplate reader (Synergy™ H1 model, BioTek Instruments, Inc.). The plate was incubated at room temperature

with 3 s shaking before each cycle of reading, and ratiometric absorbance data (Abs_{600}/Abs_{520}) were recorded over 1 h with 1-min intervals between each cycle. Measurements were done in duplicate. Duplicate ratiometric values at 10 min were averaged and plotted against peptide concentrations, and the standard error of means was shown as error bars.

8. LoD measurement

The M^{pro} was spiked into phosphate buffered (10 mM, pH 8.0) to reach a final $c_{M^{pro}}$ of 0, 1, 2, 5, 10, 20, 30, 40, 50, 100 nM (*i.e.*, with respect to a 120 μ L volume). The intact Mega peptide (13.4 μ L, 447 μ M) was then added to the mixtures in microtubes and the total volume was brought to 20 μ L using the test media. These mixtures were flicked, centrifuged, and incubated at 37 °C for 3 h. The reaction was then transferred into a 96-well plate and incubated with BSPP-AuNPs (100 μ L, 3.4 nM). The plate was incubated at room temperature in a hybrid multi-mode microplate reader with 3 s of shaking before each cycle of reading, and ratiometric absorbance data (Abs_{600}/Abs_{520}) were recorded over 1 h with 1 min intervals between each cycle. Measurements were done in duplicate. Duplicate ratiometric values at 1 h readout time were averaged and plotted against M^{pro} concentrations; error bars represent the standard error of the means. The LoD calculation follows a reported statistical method:¹¹

$$LoD_{int.} = \text{mean}_{\text{blank}} + 1.645 * (SD_{\text{blank}}) + 1.645 * (SD_{\text{low concentration sample}}) \quad (S3)$$

9. References

1. Zhang, L.; Lin, D.; Sun, X.; Curth, U.; Drosten, C.; Sauerhering, L.; Becker, S.; Rox, K.; Hilgenfeld, R., Crystal structure of SARS-CoV-2 main protease provides a basis for design of improved ketoamide inhibitors. *Science* **2020**, *368*, 409-412.
2. Mellott, D. M.; Tseng, C.-T.; Drelich, A.; Fajtová, P.; Chenna, B. C.; Kostomiris, D. H.; Hsu, J.; Zhu, J.; O'Donoghue, A. J.; McKerrow, J. H., A cysteine protease inhibitor blocks SARS-CoV-2 infection of human and monkey cells. *bioRxiv* **2020**, 2020.10.23.347534.
3. Jin, Z.; Sugiyama, Y.; Zhang, C.; Palui, G.; Xin, Y.; Du, L.; Wang, S.; Dridi, N.; Mattoussi, H., Rapid photoligation of gold nanocolloids with lipoic acid-based ligands. *Chem. Mater.* **2020**, *32*, 7469-7483.
4. Turkevich, J.; Stevenson, P. C.; Hillier, J., A study of the nucleation and growth processes in the synthesis of colloidal gold. *Discuss. Faraday Soc.* **1951**, *11*, 55-75.
5. Liu, X.; Atwater, M.; Wang, J.; Huo, Q., Extinction coefficient of gold nanoparticles with different sizes and different capping ligands. *Colloids Surf. B Biointerfaces* **2007**, *58*, 3-7.

6. Anthis, N. J.; Clore, G. M., Sequence-specific determination of protein and peptide concentrations by absorbance at 205 nm. *Protein Sci.* **2013**, *22*, 851-8.
7. Jin, Z.; Mantri, Y.; Retout, M.; Cheng, Y.; Zhou, J.; Jorns, A.; Fajtova, P.; Yim, W.; Moore, C.; Xu, M.; Creyer, M. N.; Borum, R. M.; Zhou, J.; Wu, Z.; He, T.; Penny, W. F.; O'Donoghue, A. J.; Jokerst, J. V., A Charge-Switchable Zwitterionic Peptide for Rapid Detection of SARS-CoV-2 Main Protease. *Angew. Chem. Int. Ed.* **2022**, *61*, e202112995.
8. Jin, Z.; Yeung, J.; Zhou, J.; Cheng, Y.; Li, Y.; Mantri, Y.; He, T.; Yim, W.; Xu, M.; Wu, Z.; Fajtova, P.; Creyer, M. N.; Moore, C.; Fu, L.; Penny, W. F.; O'Donoghue, A. J.; Jokerst, J. V., Peptidic Sulfhydryl for Interfacing Nanocrystals and Subsequent Sensing of SARS-CoV-2 Protease. *Chem. Mater.* **2022**, *34*, 1259-1268.
9. Rodbard, D.; Chrambach, A., Unified Theory for Gel Electrophoresis and Gel Filtration. *Proc. Natl. Acad. Sci. U.S.A.* **1970**, *65*, 970-977.
10. Johnston, B. D.; Kreyling, W. G.; Pfeiffer, C.; Schäffler, M.; Sarioglu, H.; Ristig, S.; Hirn, S.; Haberl, N.; Parak, W. J., Colloidal Stability and Surface Chemistry Are Key Factors for the Composition of the Protein Corona of Inorganic Gold Nanoparticles. *Adv. Funct. Mater.* **2017**, *27*, 1701956.
11. Armbruster, D. A.; Pry, T., Limit of blank, limit of detection and limit of quantitation. *Clin. Biochem. Rev.* **2008**, *29 Suppl 1*, S49-S52.
12. Chang, Y.-C.; Jin, Z.; Li, K.; Zhou, J.; Yim, W.; Yeung, J.; Creyer, N. M.; Fajtová, P.; He, T.; Chen, X.; O'Donoghue, J. A.; Jokerst, J. V., Peptide valence-induced break in plasmonic coupling. *Chem. Sci.* **2023**, accepted article.

Supporting Figures

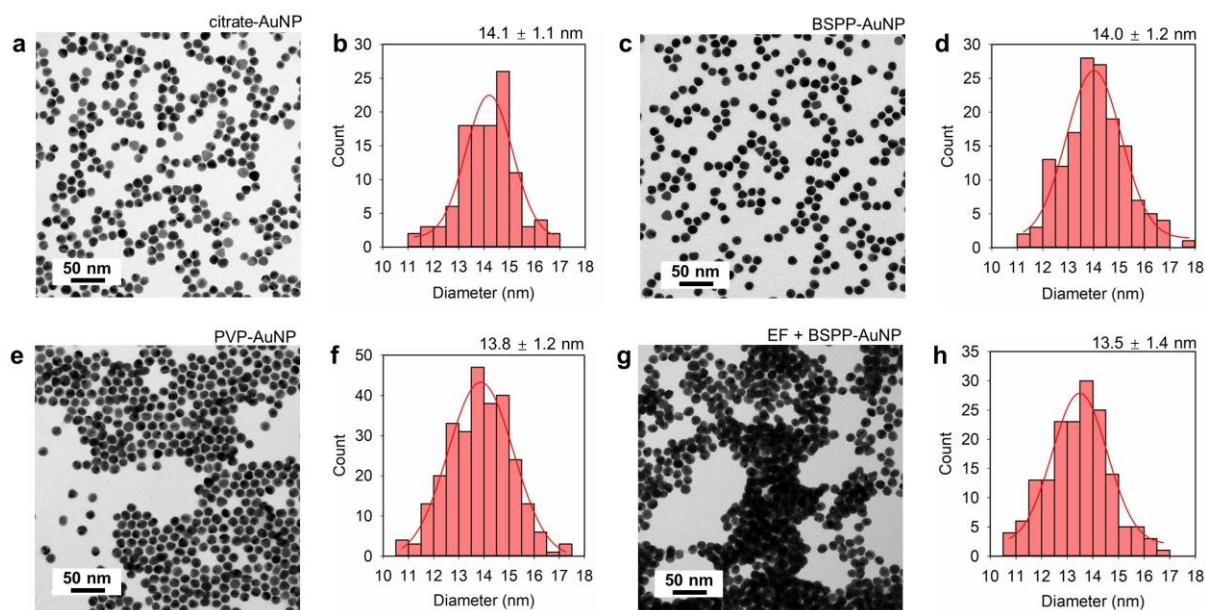


Figure S1. TEM images of the representative AuNPs. (a) The as-prepared citrate-AuNPs and (b) a histogram of particle size with an average diameter of 14.1 ± 1.1 nm. (c) The BSPP-AuNPs with (d) a diameter of 14.0 ± 1.2 nm. (e) The PVP-AuNPs with (f) a diameter of 13.8 ± 1.2 nm. (g) The BSPP-AuNPs incubated with $50 \mu\text{M}$ EF peptide with (h) a diameter of 13.5 ± 1.4 nm. Data were analyzed in ImageJ by counting more than 100 particles using a manual size method.

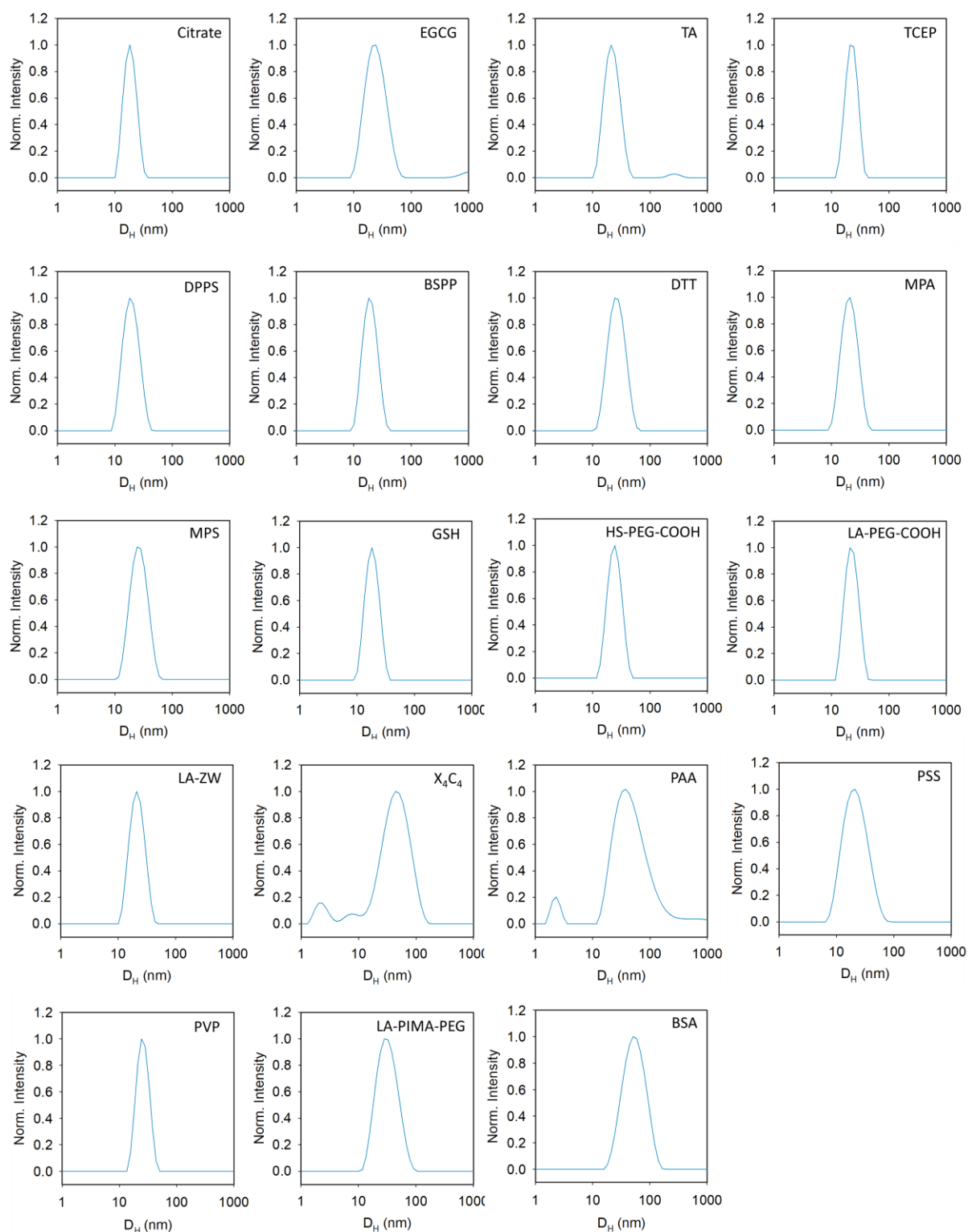


Figure S2. Hydrodynamic diameter (D_H) distributions obtained from dynamic light scattering of ligated AuNPs. The values and polydispersity index (PDI) are listed in **Table 1**.

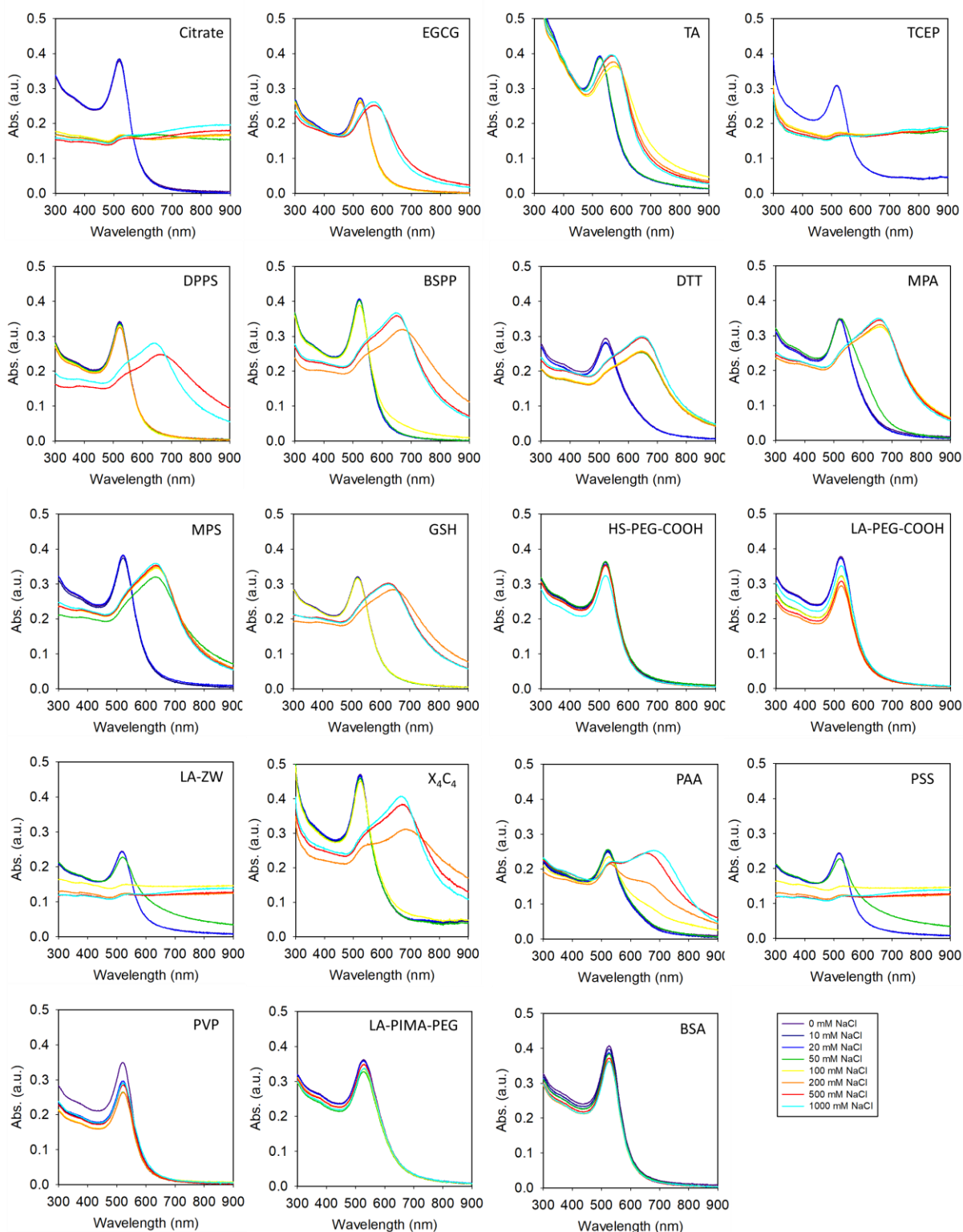


Figure S3. Absorption spectra of AuNPs capped with different ligands when incubated with various concentrations (0, 10, 20, 50, 100, 200, 500, and 1000 mM) of NaCl solution for 10 minutes.

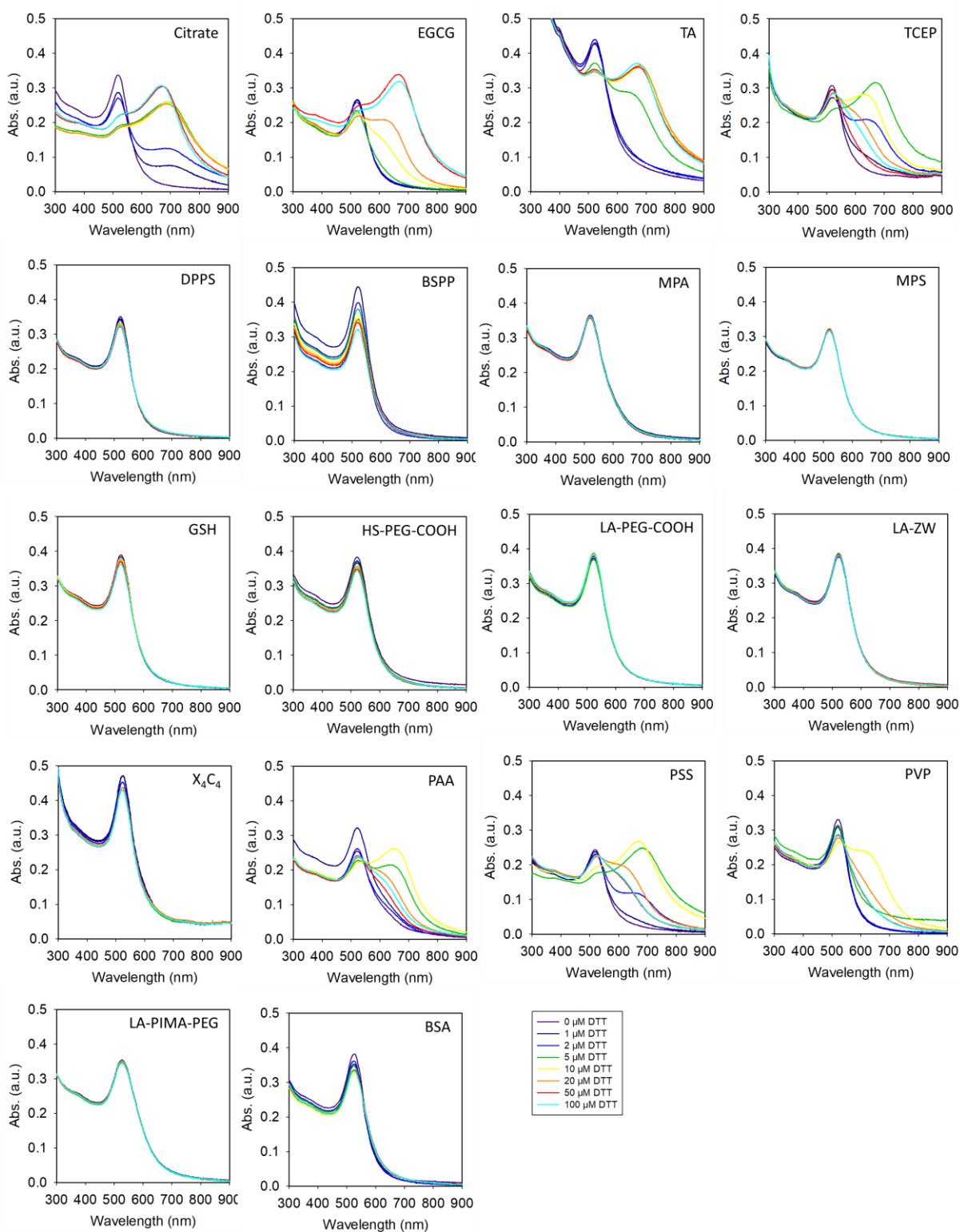


Figure S4. Absorption spectra of AuNPs capped with different ligands when incubated with various concentrations (0, 1, 2, 5, 10, 20, 50, and 100 μM) of dithiothreitol (DTT) solution for 10 minutes. Note that all the DTT solution contains 10 mM of NaCl to promote the covalent aggregation of AuNPs.

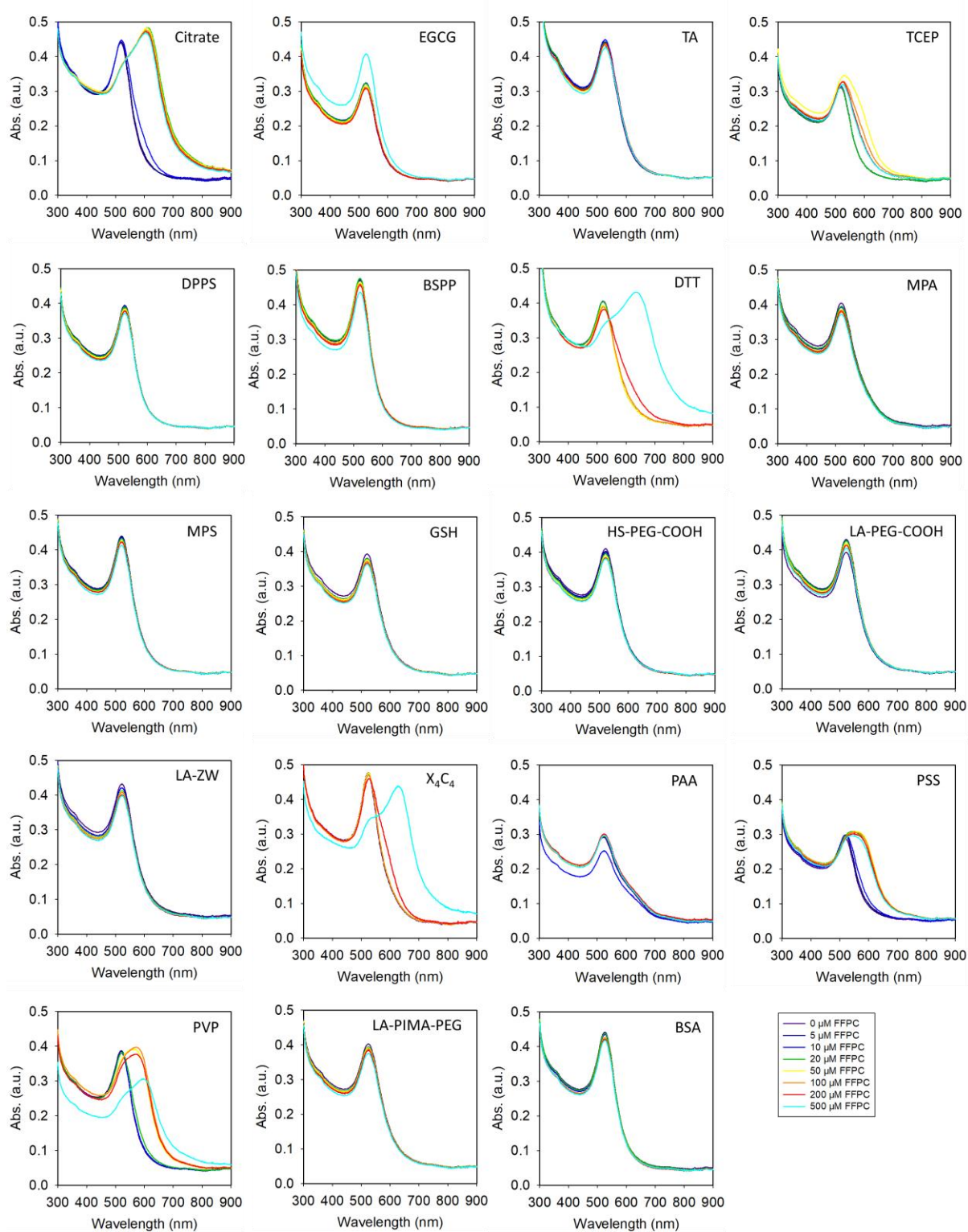


Figure S5. Absorption spectra of AuNPs capped with different ligands when incubated with various concentrations (0, 5, 10, 20, 50, 100, 200, and 500 μM) of amphiphilic FFPC peptide solution for 10 minutes.

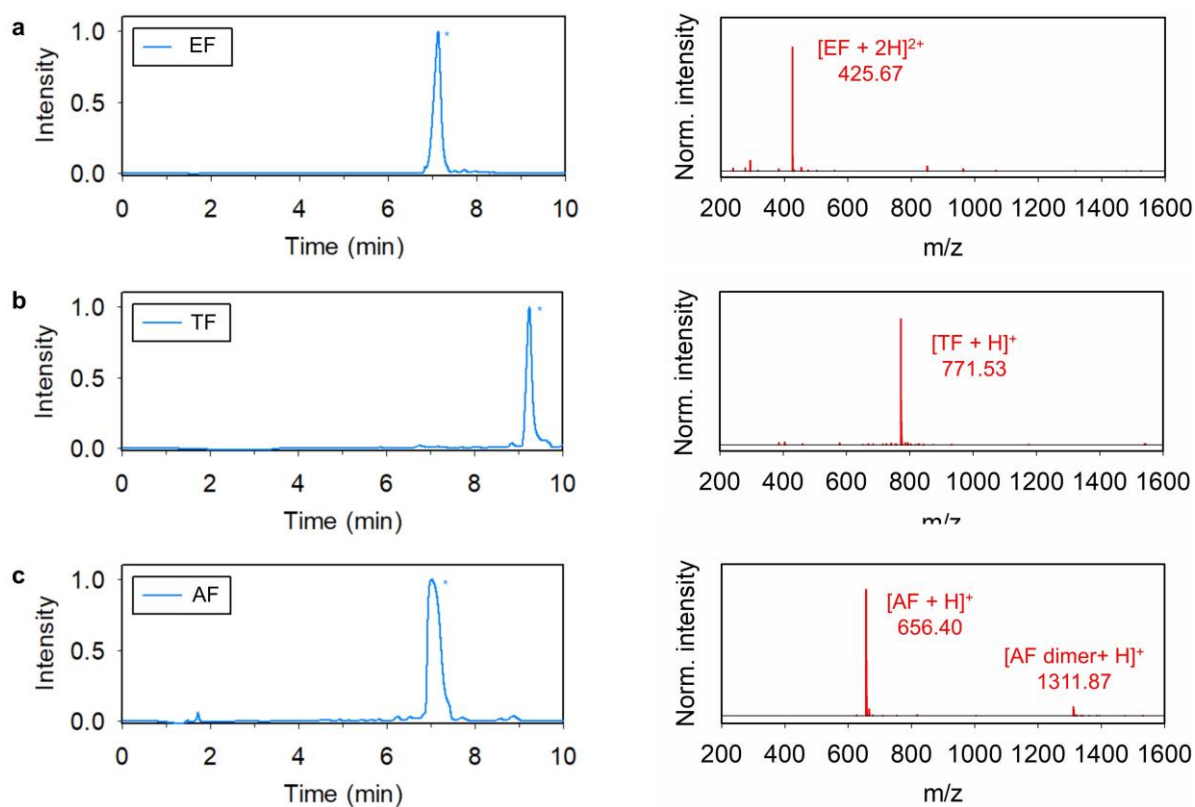


Figure S6. HPLC and ESI-MS data of the peptide segments including (a) EF, (b) TF, and (c) AF. The peptide information can be found in **Table 2**. $[\text{EF}+2\text{H}]^{2+}/2$ calcd. for 425.22; found, 425.67. $[\text{TF}+\text{H}]^+$ calcd. for 771.28; found, 771.53. $[\text{AF}+\text{H}]^+$ calcd. for 656.28; found, 656.40.

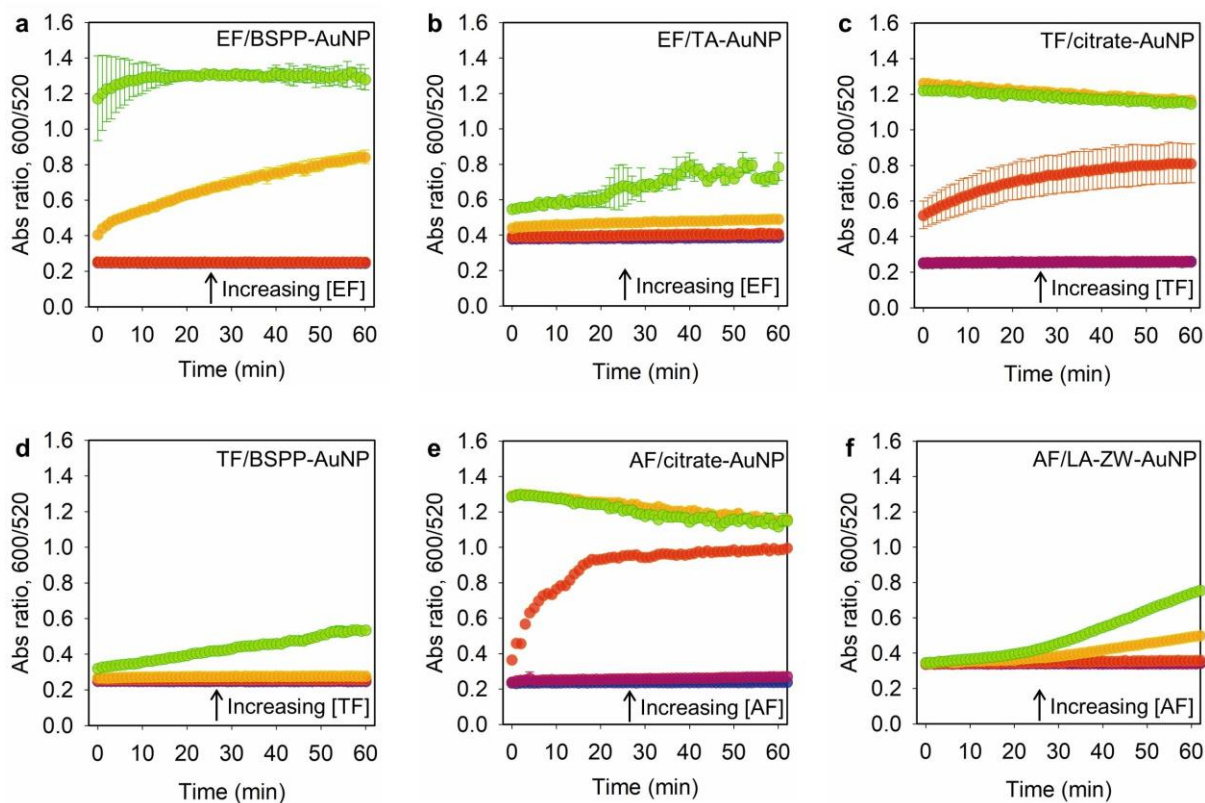


Figure S7. Time-dependent aggregation kinetics of the ligated AuNPs in the presence of peptide fragments for over 1 h. Absorbance ratio (Abs_{600}/Abs_{520}) of (a) EF peptide mixed with BSPP-AuNPs, (b) EF peptide mixed with tannic acid-AuNPs, (c) TF peptide mixed with citrate-AuNPs, and (d) TF peptide mixed with BSPP-AuNPs. (e) AF peptide mixed with citrate-AuNPs, and (f) AF peptide mixed with LA-ZW-AuNPs. Each plot shows five peptide concentrations from 0.1, 0.5, 2 (red), 10 (yellow), 50 (green) μM . Error bars = standard deviations ($n = 3$). The data points at 10 min were extracted for analyzing the critical coagulation concentration (CCC).

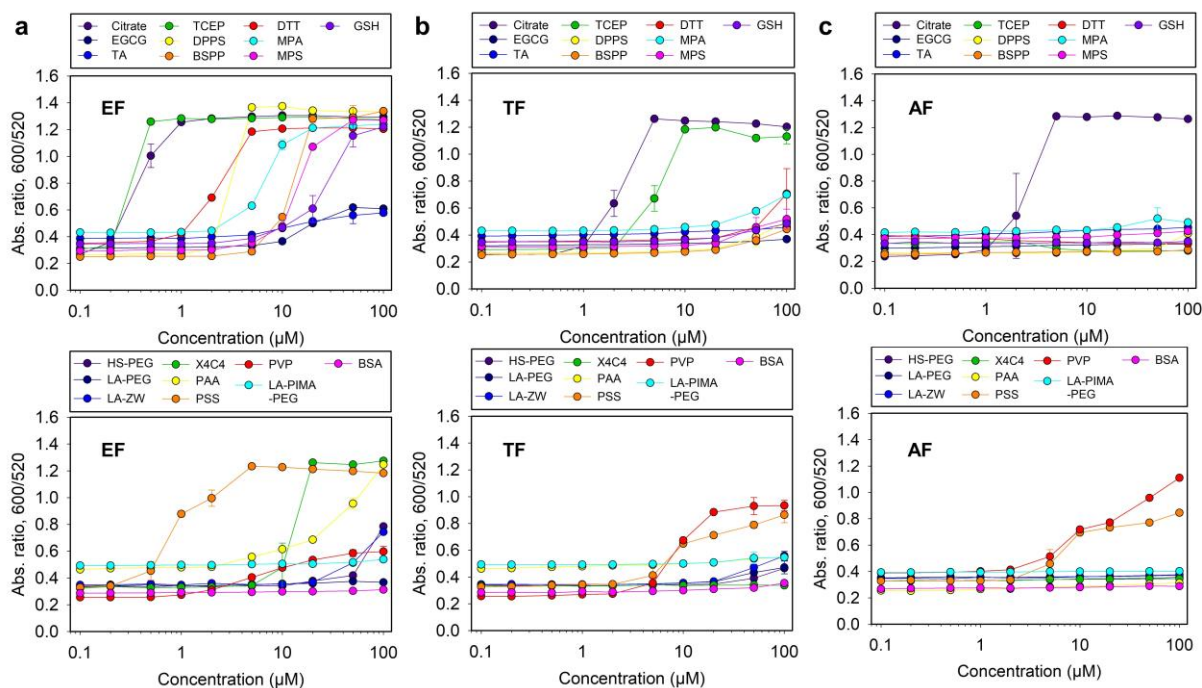
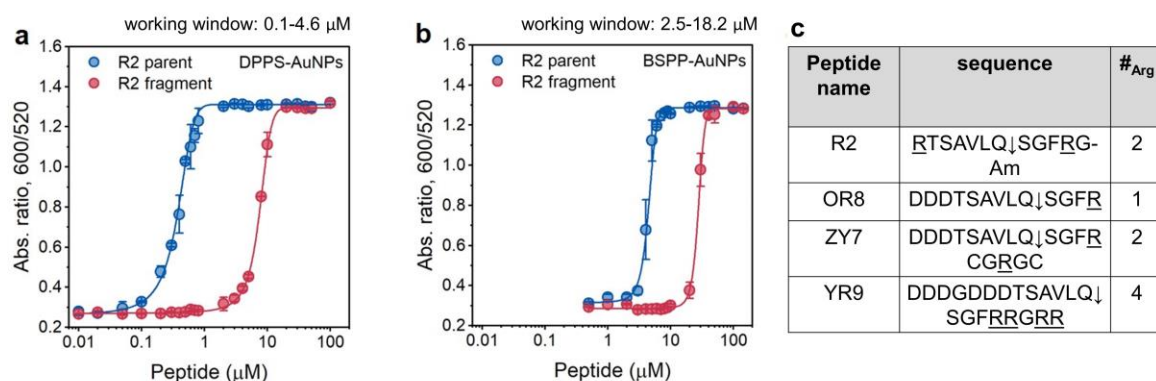


Figure S8. Concentration-dependent absorbance ratio (Abs_{600}/Abs_{520}) of the ligated AuNPs after incubating with the (a) EF, (b) TF, and (c) AF peptides for 10 minutes. The critical coagulation concentration (CCC) is defined as the first concentration of signal jump and is summarized in **Table 3**. The EF segment aggregates the AuNPs coated with citrate, EGCG, TA, TCEP, DPPS, BSPP, DTT, MPA, MPS, X₄C₄, PAA, and PSS molecules. The TF segment aggregates the AuNPs coated with citrate, TCEP, PVP, and PSS molecules. The AF segment aggregates the AuNPs coated with citrate, PVP, and PSS molecules.

(i) Effect of NP colloidal stability on working window



(ii) Effect of peptide charge valence on working window

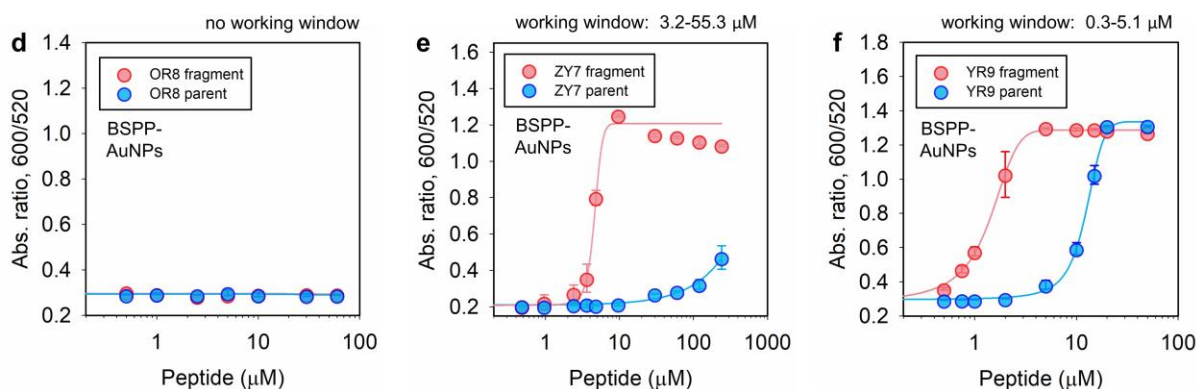


Figure S9. The choice of a peptide/AuNP pair as a good color sensor is determined by the charge valence of counterions and the matched colloidal stability. Working windows of M^{PRO} sensors based on ratiometric signal ($\text{Abs}_{600}/\text{Abs}_{520}$) collected from (a) DPPS-AuNPs, and (b) BSPP-AuNPs incubated with various amounts of R2 parent (blue) and fragments (red), respectively. For peptide charge valence of 2 (i.e., R2 peptide), BSPP-AuNPs of higher colloidal stability showed a wider working window than that of the DPPS-AuNPs of weaker colloidal stability, e.g., 2.5-18.2 μM versus 0.1-4.6 μM .¹² (d) When peptide of one positive charge valence [i.e., #_{Arg} = 1 for OR8 peptide, sequence in DDDTSAVLQ↓SGFR] is combined use with BSPP-AuNPs, both parent and fragment could not induce aggregation due to the mismatched colloidal stability of BSPP-AuNPs, that is, effective working window does not exist. (e) When peptide of two positive charge valence [i.e., #_{Arg} = 2 for ZY7 peptide, sequence in DDDTSAVLQ↓SGFRCRGC] is combined use with BSPP-AuNPs, a large working window is resulted due to the matched colloidal stability of BSPP-AuNPs. (f) When peptide of four positive charge valence [i.e., #_{Arg} = 4 for YR9 peptide, sequence in DDDGDDDTSAVLQ↓SGFRRRGRR] is combined use with BSPP-AuNPs, a narrow-or-no effective working window is resulted due to the mismatched colloidal stability of BSPP-AuNPs. The peptide information is shown in panel c. The low and high limit of working window are

determined by eq (S3). **Panels a-b** are reprinted with permission from ref. 12. Copyright (2023) Royal Society of Chemistry. **Panels d-f** are reprinted with permission from ref. 7. Copyright (2022) Wiley-VCH Verlag GmbH & Co. KGaA.

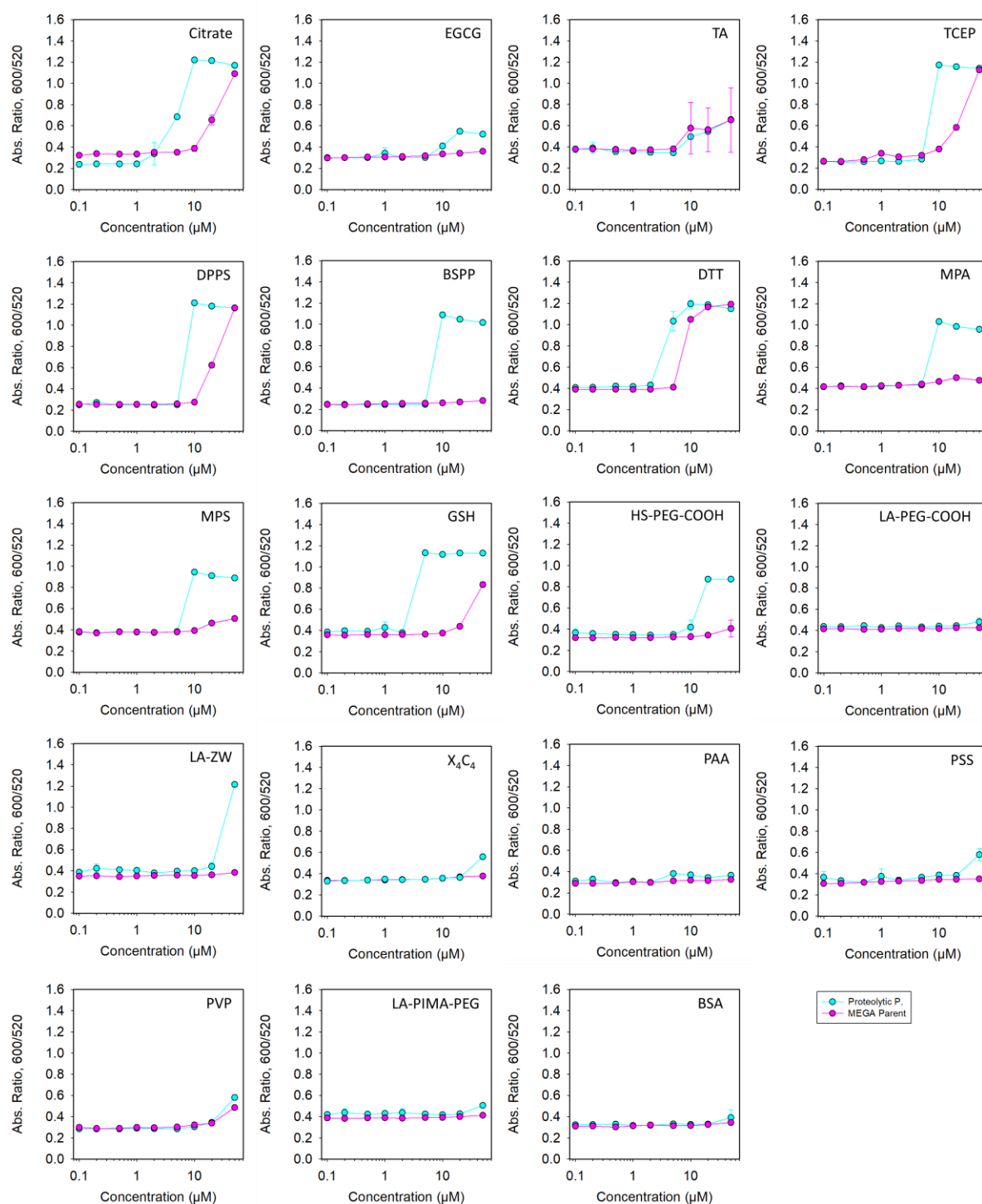


Figure S10. Working window of Mega peptide containing two Arg, Cys, and Phe residues with different ligated AuNPs. The parent peptide (purple curve) was incubated with M^{Pro} at 37°C

overnight to ensure that the peptide is fully cleaved (cyan curve). The AuNPs capped with citrate, DPPS, BSPP, MPA, MPS, GSH, HS-PEG-COOH, LA-ZW, X₄C₄, and PSS all have good sensing values.

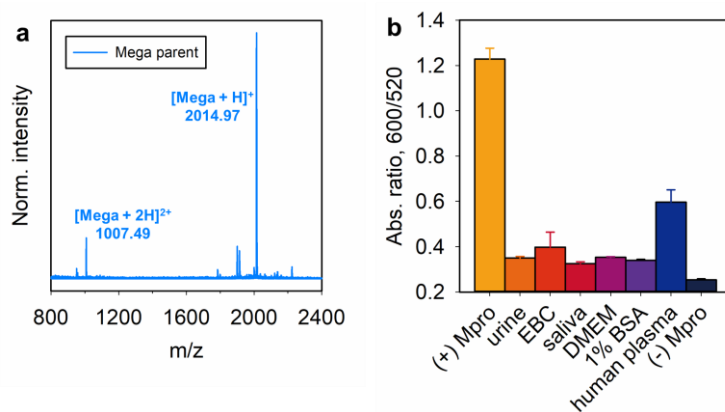


Figure S11. (a) ESI-MS data of intact Mega peptide. (b) The stability of BSPP-AuNPs (3.4 nM, 100 μ L) in different matrix media (20 μ L). Positive control used tris buffer with M^{pro}. The negative control used tris buffer without M^{pro}. The BSPP-AuNPs showed little color change in human plasma.

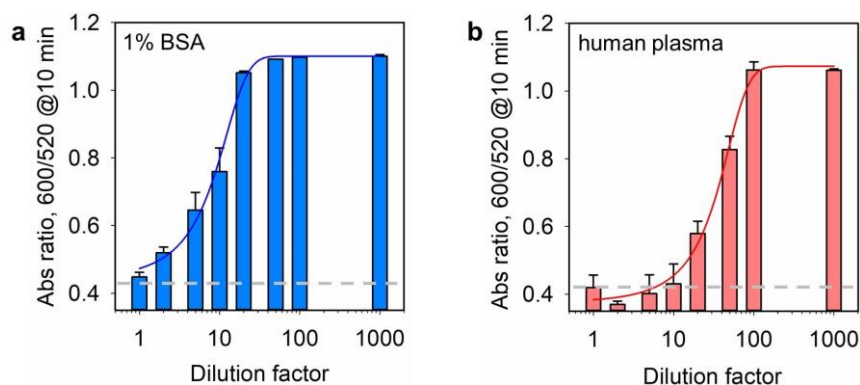


Figure S12. Dilution factor required for inducing color changes in (a) 1% w/v BSA and (b) human plasma. The dilution factors used 1×, 2×, 5×, 10×, 20×, 50×, 100×, and 1000×. The procedure follows the protocol in **Section 8**, Supporting Information, and Mega peptide (50 μM), M^{Pro} (50 nM), and BSPP-AuNPs (3.4 nM, 100 μL) were used. A dilution factor of 5× is optimal for aggregation in 1% BSA, and a dilution factor of 20× is optimal for the human plasma matrix. The dash grey line indicates the base line where no aggregation or color change occurs.

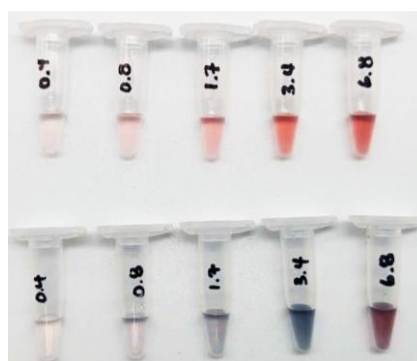


Figure S13. Concentration optimization of the 13-nm AuNPs for aggregation-based colorimetric assays. Citrate-AuNPs (100 μL) and NaCl (5 μL, 150 mM) were used for the experiments. The tested concentrations from left to right are 0.4, 0.8, 1.7, 3.4, and 6.8 nM. We chose 3.4 nM as the optimal NP concentration for the sake of reducing the amount of aggregants (or titrants) used for aggregation, while still giving intense and visible color changes.